Annals of Forest Science (2019) 76: 115
https://doi.org/10.1007/s13595-019-0905-0

RESEARCH PAPER

Large hydraulic safety margins protect Neotropical canopy rainforest tree species against hydraulic failure during drought

Camille Ziegler[1,2] · Sabrina Coste[3] · Clément Stahl[2] · Sylvain Delzon[4] · Sébastien Levionnois[5] · Jocelyn Cazal[2] · Hervé Cochard[6] · Adriane Esquivel-Muelbert[7,8] · Jean-Yves Goret[2] · Patrick Heuret[9] · Gaëlle Jaouen[10] · Louis S. Santiago[11,12] · Damien Bonal[1]

Received: 8 July 2019 / Accepted: 18 November 2019 / Published online: 11 December 2019

Abstract

• ***Key message*** Abundant Neotropical canopy-tree species are more resistant to drought-induced branch embolism than what is currently admitted. Large hydraulic safety margins protect them from hydraulic failure under actual drought conditions.

• ***Context*** Xylem vulnerability to embolism, which is associated to survival under extreme drought conditions, is being increasingly studied in the tropics, but data on the risk of hydraulic failure for lowland Neotropical rainforest canopy-tree species, thought to be highly vulnerable, are lacking.

• ***Aims*** The purpose of this study was to gain more knowledge on species drought-resistance characteristics in branches and leaves and the risk of hydraulic failure of abundant rainforest canopy-tree species during the dry season.

• ***Methods*** We first assessed the range of branch xylem vulnerability to embolism using the flow-centrifuge technique on 1-m-long sun-exposed branches and evaluated hydraulic safety margins with leaf turgor loss point and midday water potential during normal- and severe-intensity dry seasons for a large set of Amazonian rainforest canopy-tree species.

• ***Results*** Tree species exhibited a broad range of embolism resistance, with the pressure threshold inducing 50% loss of branch hydraulic conductivity varying from − 1.86 to − 7.63 MPa. Conversely, we found low variability in leaf turgor loss point and dry season midday leaf water potential, and mostly large, positive hydraulic safety margins.

DB and SC should be considered joint senior authors

Handling Editor: Andrew Merchant

Contributions of the co-authors: Authors' contribution Conceived and designed the experiments: CZ, SC, CS, LS, and DB; acquired data: CZ, SC, CS, SD, SL, PH, JYG, and JC; managed forest inventory data: GJ; analyzed the data: CZ, SC, CS, and DB; wrote the first draft of the paper: CZ, SC, CS, and DB. All authors read and approved the final manuscript.

✉ Damien Bonal
damien.bonal@inra.fr

Camille Ziegler
camille.ziegler@ecofog.gf

Sabrina Coste
sabrina.coste@ecofog.gf

Clément Stahl
clement.stahl@ecofog.gf

Sylvain Delzon
pujoulade@gmail.com

Sébastien Levionnois
sebastien.levionnois@ecofog.gf

Jocelyn Cazal
jocelyn.cazal@ecofog.gf

Hervé Cochard
herve.cochard@inra.fr

Adriane Esquivel-Muelbert
a.esquivelmuelbert@bham.ac.uk

Jean-Yves Goret
jean-yves.goret@ecofog.gf

Patrick Heuret
patrick.heuret@inra.fr

Gaëlle Jaouen
gaelle.jaouen@ecofog.gf

Louis S. Santiago
louis.santiago@ucr.edu

Extended author information available on the last page of the article

INRA SCIENCE & IMPACT · Springer

• ***Conclusions*** Rainforest canopy-tree species growing under elevated mean annual precipitation can have high resistance to embolism and are more resistant than what was previously thought. Thanks to early leaf turgor loss and high embolism resistance, most species have a low risk of hydraulic failure and are well able to withstand normal and even severe dry seasons.

Keywords Amazon rainforest · Embolism resistance · Hydraulic safety margins · Turgor loss point · Water potential

1 Introduction

Tropical rainforest ecosystems are characterized by high annual rainfall. Yet, most Amazonian rainforests are regularly exposed to seasonal droughts due to the latitudinal movements of the Intertropical Convergence Zone (Bonal et al. 2016). Reduced soil water availability due to low precipitation during the dry season can cause a reduction in tree growth (Wagner et al. 2012), photosynthetic assimilation, and whole-tree transpiration due to stomatal closure (Stahl et al. 2013). Increased mortality can occur with increasingly severe dry seasons (Phillips et al. 2010) and species exhibiting contrasting drought-resistance characteristics are likely to be affected differently (Anderegg et al. 2016). This indicates that drought resistance may provide an advantage for tropical trees under climate change and that droughts are likely to alter tree species' distribution as well as community composition and functioning (Esquivel-Muelbert et al. 2019). Furthermore, little is known about the trait syndromes that confer drought resistance in tropical rainforests or how they participate in shaping species distribution along macro-environmental gradients of water availability (Zhu et al. 2018).

Assessing tropical rainforest species and community resistance to drought in a context of increasingly frequent severe dry seasons (Duffy et al. 2015) requires a deep understanding of the mechanisms enabling the maintenance of physiological functions, and hence survival, during periods of low water availability (Anderegg et al. 2015). Tree species display a variety of drought tolerance and drought avoidance strategies (Delzon 2015), especially in hyper-diverse tropical rainforests (Santiago et al. 2016). Therefore, using traits to describe these strategies may be particularly helpful in predicting whether a given species will be able to withstand future climatic conditions which could potentially alter its present bioclimatic distribution range.

Loss of hydraulic conductivity leading to xylem hydraulic failure and plant desiccation has been identified as an important mechanism involved in drought-induced tree mortality (Adams et al. 2017). Therefore, the spread of branch embolism during drought could not only have an impact on the overall fitness of individual trees but could also affect tree community functioning. Plants can, however, avoid hydraulic failure through the expression of several hydraulic traits. Plant xylem vulnerability to embolism—expressed as the xylem pressure at which 50% of branch hydraulic conductivity is lost (Ψ_{50}; MPa)—is an adaptive (Maherali et al. 2004) and mechanistic trait with strong predictive power for plant survival and distribution (Urli et al. 2013; Anderegg et al. 2015; Brodribb 2017). Embolism resistance varies with mean annual precipitation at the inter-biome scale (Maherali et al. 2004; Choat et al. 2012) and with water availability at the local scale (Oliveira et al. 2019). Species with more negative Ψ_{50} values are able to tolerate more negative water potentials and sustain hydraulic conductivity and can therefore thrive in drier conditions (Choat et al. 2018). The xylem hydraulic safety margin (HSM; MPa), expressed as the difference between seasonal minimum xylem water potential and Ψ_{50}, was found to better explain mortality during severe droughts than Ψ_{50} alone or than other traits (Anderegg et al. 2016). In a meta-analysis, Choat et al. (2012) showed that trees typically operate at positive HSM, indicating that they are not being routinely exposed to high levels of branch embolism. Yet, Choat et al. (2012) reported converging, narrow HSM values (< 1 MPa) among biomes for Angiosperm species, suggesting that forests will be highly vulnerable to an increase in the frequency of severe droughts. During moderate droughts, some species have the ability to preserve leaf functioning (i.e., growth, gas exchange, leaf hydraulic conductance) thanks to a lower leaf water potential at which leaf cells lose turgor (henceforth denoted π_{tlp}; MPa; Bartlett et al. 2012a, b). With increasing drought intensity, leaf water potential decreases to and past π_{tlp}, mediating stomatal closure and thereby limiting leaf transpiration and the consequential further decrease in water potential (Brodribb et al. 2003; Bartlett et al. 2016). As a consequence, π_{tlp} has been used as an indicator for stomatal behavior (Mencuccini et al. 2015) and as a proxy for stomatal closure during drought (Martin-StPaul et al. 2017; Hochberg et al. 2018).

These hydraulic traits can act in concert or as a result of trade-offs that determine plant drought resistance, which can be attained through multiple strategies (Pivovaroff et al. 2016). It is therefore paramount to consider drought resistance strategies in terms of interactions among traits expressed in different organs. The longstanding view that Ψ_{50} and π_{tlp} are coordinated to maintain leaf functioning and productivity under drought stress (Jones and Sutherland 1991) has recently been challenged (Mencuccini et al. 2015; Martin-StPaul et al. 2017). Indeed, π_{tlp} was much less variable and in most cases less negative than Ψ_{50} along the global spectrum of Ψ_{50} variations. The same pattern was found in another meta-analysis for ~ 80% of tropical rainforest tree species for which sigmoidal vulnerability curves were selected (Bartlett et al. 2016). This indicates that (i) trees generally have a positive hydraulic safety margin between stomatal closure (π_{tlp}) and the spread of embolism (Ψ_{50}) and that (ii) stomata must close in order

to avoid the rapid spread of branch embolism and subsequent hydraulic failure.

Over the past decades, a tremendous effort has been made to improve our understanding of the mechanisms of plant response and resistance to drought in various biomes. Yet, a major knowledge gap still remains for tropical rainforest tree species (Bonal et al. 2016). These species, which typically experience high precipitation regimes, are believed to have low intra-biome variation and less negative Ψ_{50} values (i.e., higher vulnerability to drought-induced branch xylem embolism) than those in drier forest biomes (Maherali et al. 2004; Choat et al. 2012). Unfortunately, the data available for Amazonian rainforest canopy-tree species are limited and some are subject to methodological doubt (see Torres-Ruiz et al. 2016 concerning Rowland et al. 2015). Tropical rainforests also represent the woody-biome with the least negative mean π_{tlp} values observed so far (Bartlett et al. 2012a, b; Zhu et al. 2018), reinforcing the claim that rainforest tree species cannot tolerate strong declines in water potential without closing their stomata (Fisher et al. 2006). However, π_{tlp} showed significant interspecific variation for Amazonian rainforest canopy-tree species in French Guiana (Marechaux et al. 2015), which extends the expected range for tropical rainforest canopy tree species. Moreover, species identity was shown to be the main driver of variation in π_{tlp}, with, respectively, low and negligible intraspecific and seasonal variability (Maréchaux et al. 2016). At present, the few studies providing a combined investigation of Ψ_{50} and π_{tlp} for tropical rainforest species concern only a limited number of species and have yielded contradictory conclusions (Mencuccini et al. 2015; Nolf et al. 2015; Bartlett et al. 2016; Martin-StPaul et al. 2017; Powell et al. 2017). Likewise, the absence of a general consensus on the magnitude of Ψ_{50} and the risk of hydraulic failure in hyper-diverse ecosystems such as tropical rainforests highlights the need for more research, in particular for large canopy–trees, which are at higher risk of drought-induced mortality during extreme climatic events (Bennett et al. 2015).

We assessed the vulnerability of rainforest tree species to drought-induced branch xylem embolism and the risk of hydraulic failure under normal- and severe-intensity dry seasons. We explored interspecific variability and covariations in branch and leaf hydraulic traits known to be important in drought response and survival. Xylem branch vulnerability to embolism, leaf water potential at turgor loss point, and midday leaf water potential were estimated in 30 co-occurring rainforest canopy-tree species in French Guiana. With this unique set of hydraulic traits, we addressed the following questions:

(i) What is the range of variation in branch xylem vulnerability to embolism in abundant, co-occurring lowland tropical rainforest canopy-tree species?

(ii) Are these species exposed to a risk of hydraulic failure during normal and severe droughts?

2 Materials and methods

2.1 Study site and species selection

The fieldwork was conducted at Paracou Research Station (https://paracou.cirad.fr; 5°16′26″N, 52°55′26″W) in a lowland tropical rainforest of the Guiana Shield in French Guiana. The site has a mean (± SE) annual air temperature of 25.7 °C ± 0.1 °C and a mean precipitation of 3102 mm ± 70 mm (from 2004 to 2014; Aguilos et al. 2019) with a dry season typically occurring from mid-August to mid-November. During this dry season, precipitation can be less than 50 mm/month and soil water availability is strongly reduced (< 0.4; Aguilos et al. 2019). The forest is characterized by a succession of small hills (up to 40 m a.s.l) comprising plateaus and slopes as well as seasonally flooded areas.

The study was conducted at the Paracou experimental site, managed by CIRAD, in plots 6, 11, and 15, each of which are 6.25 ha of undisturbed forest. All trees ≥ 10 cm in diameter within the plots have been tagged, mapped, identified to species level, and annually or biennially measured for diameter growth for about 30 years. Based on total basal area by species in this botanical inventory data, we selected the most common canopy-tree species present on plateaus or moderate slopes (*terra firme*) at the site. The sampling included the three main commercial species (*Dicorynia guianensis*, *Qualea rosea*, and *Sextonia rubra*), which account for 71.7% of the logging volume in French Guiana (Fargeon et al. 2016).

We sampled branches and leaves of co-occurring canopy-tree species belonging to 11 botanical families (Table 3 in the Appendices) of which Burseraceae, Chrysobalanaceae, Fabaceae, Lecythidaceae, and Sapotaceae were the most represented in our sample. Thirty tree species were investigated, eight of which produce exudates (Table 7 in the Appendices). We selected healthy dominant or co-dominant canopy trees. Only one understory species (*Gustavia hexapetala*) was selected. Accessibility for tree climbers to sunlit leaves or branches was also a selection criterion.

We measured leaf traits on 29 species and the hydraulic characteristics of the branches supporting these leaves for 25 species (Table 4 in the Appendices). The latter measurements were conducted on three to ten individuals per species (Table 4 in the Appendices), with exceptions for seven species out of the total 25 for which we could obtain only one or two vulnerability curves. Branch hydraulics could not be obtained for four species: *Licania alba* and *Licania heteromorpha* had extremely long maximum vessel lengths and were not measured (see *Vulnerability curves*); we did not succeed in

measuring *Vouacapoua americana* despite repeated attempts; and too few *Sextonia rubra* individuals were sampled to yield results. Leaf traits could not be obtained for two species: the only *Protium sagotianum* individual on which branches were sampled died; and the dense secondary vein network of *Qualea rosea* hampered an accurate determination of turgor loss point (Maréchaux, Bartlett et al. 2016).

2.2 Vulnerability curves

Professional tree climbers sampled 2–3-m-long, sun-exposed canopy branches with a diameter under bark ranging from 8.7 to 18.2 mm during the rainy season, i.e., between January and July 2017. While sampling the branches, the climbers attached strings to nearby fine, sun-exposed twigs so that they could later be pulled down for leaf sampling. After sampling, the branches intended for the determination of branch xylem vulnerability to embolism were immediately defoliated to prevent transpiration loss, recut under water, conditioned in wet cloth, and sealed in heavy-duty black plastic bags to halt moisture loss (Delzon et al. 2010). They were taken to the laboratory in Kourou (a 45-min drive), recut to 1.5 m in length, reconditioned in damp absorbent paper with both ends covered in plastic wrap, sealed with tape inside heavy-duty plastic bags, and immediately sent by priority transport (1–2 days) to the Caviplace phenotyping platform (Genebois, Univ. of Bordeaux, Pessac, France).

Prior to final measurements, the branches were recut under water to a length of 1 m and debarked at both ends to help limit the amount of exuded mucilage. Vulnerability to embolism was measured following the flow-centrifugation technique (Cochard et al. 2013) in a large Cavitron equipped with a 1-m diameter custom-built rotor (Cavi1000; DGMeca, Gradignan, France). This large rotor was designed to process species with long vessels (Lobo et al. 2018). This limits the occurrence of 'open-vessel' artifacts if the vessel length is much shorter than the diameter of the rotor (Cochard et al. 2013). The percentage loss of conductivity (PLC) was measured for each branch in 0.5 MPa pressure steps (Cavisoft v1.5; Univ. Bordeaux, Pessac). Vulnerability curves (VCs) were obtained by plotting increasing PLC with decreasing xylem pressure. VCs were fitted with a sigmoid function (Pammenter and Vander Willigen 1998) following the Nlin procedure in SAS (SAS 9.4, SAS Institute, Cary, NC, USA) and hydraulic traits were determined. Ψ_{50} (MPa), the xylem pressure inducing 50% loss of branch hydraulic conductivity, is a widely used metric representing the steepest point of the VC, meaning that even a small decrease in water potential will cause a substantial reduction in hydraulic conductivity (Maherali et al. 2004; Choat et al. 2012). a_x (%MPa^{-1}) is the slope of the VC at the inflexion point and is a good indicator of the speed at which embolism affects the stem (Delzon et al. 2010). Additionally, we obtained the xylem pressures inducing 12% (Ψ_{12}; MPa) and 88% (Ψ_{88}; MPa) loss of branch hydraulic conductivity. Ψ_{12} corresponds to the water potential which reflects the initial air-entry producing embolism (Meinzer et al. 2009), while Ψ_{88} is thought to be the xylem water potential threshold above which hydraulic damage may be irreversible, leading to high levels of tree mortality in Angiosperm tree species (Choat et al. 2012; Urli et al. 2013).

We also measured the maximum vessel length (MVL; cm; Table 7 in the Appendices) in canopy branches of similar dimensions from the same trees sampled for the VCs, following the air-injection method (Ewers and Fisher 1989). Air was injected at a pressure of 1 kPa from the distal end of the branch while the basal end was recut underwater every 2 cm. Once the first air bubbles appeared from the cut end surface, branch length was measured with a measuring tape and MVL was recorded. We excluded species with a MVL far above 1 m for a given diameter of ca. 2 cm (i.e., *Licania alba* and *Licania heteromorpha*) and selected smaller diameter branches for species with a MVL close to 1 m (i.e., *Eperua falcata*, *Goupia glabra*, and *Licania membranacea*).

2.3 Leaf turgor loss point

Leaf water potential at turgor loss point (π_{tlp}, MPa) was estimated during the 2017 dry season on canopy leaves with a vapor pressure osmometer (VAPRO 5520, Wescor, Logan, UT, USA; Bartlett et al. 2012a, b). This method was previously validated and used in a study conducted on tropical rainforest trees in French Guiana (Maréchaux, Bartlett et al. 2016). After harvest, the leaves were immediately sealed in plastic bags containing moist absorbent paper, placed in a cooler, taken to the laboratory in Kourou and placed at 5 °C to allow them to rehydrate overnight. The next day, one 8-mm disk per leaf was sampled with a sharp cork borer, care being taken to avoid first- and second-order veins. The disk was immediately wrapped in tinfoil and frozen by immersion in liquid nitrogen (LN_2) for at least 2 min, then punctured 10–15 times with a needle and sealed in an osmometer with a standard 10-μl chamber well. The equilibrium solute concentration value C_0 (mmol kg^{-1}) was recorded from the osmometer when the difference between two consecutive measurements fell below 5 mmol kg^{-1}. A previously established linear relationship with the osmotic potential at full turgor (π_{osm}) was used to convert to π_{osm} following the van't Hoff equation relating solute concentrations to vapor pressure:

$$\pi_{osm} = \frac{2.5}{1000} \times c_o, \quad (1)$$

where the numerator of the first term represents $R \times T = 2.5$ L MPa mol^{-1} at 25 °C, with R, the ideal gas constant, and T, the temperature in degrees Kelvin. The value of π_{tlp} was then calculated from π_{osm} (Bartlett et al. 2012a, b) as

$$\pi_{tlp} = 0.832 \times \pi_{osm} - 0.631. \quad (2)$$

2.4 Dry season midday leaf water potential

Midday leaf water potential (Ψ_{md}; MPa) was measured with a pressure chamber (Model 1505D, PMS, USA) between 11:00 and 14:00 on clear sunny days with a high vapor pressure deficit (VPD = 1.32 kPa) during the 2018 dry season in early October when soil relative extractable water was low (REW = 0.21; Fig. 4 in the Appendices). The measurements were conducted on individual trees for which vulnerability curves were available and also on additional co-occurring canopy trees of the same species in order to increase sample size and reach three to five replicates per species. Additionally, we measured Ψ_{md} on four species for which we had not obtained VCs. We followed a specific protocol to ensure reliable readings of Ψ_{md} for laticiferous species exuding clear-exudates (as opposed to colored ones). When clear foam (latex plus air) appeared, usually from only a few distinct points on the petiole cross-section, it was rapidly blotted away with absorbent paper. This was repeated until a liquid (xylem water) appeared and covered the entire cross-section, then Ψ_{md} was immediately recorded.

Environmental conditions during these measurements were typical of an average-intensity (henceforth denoted "normal") dry season, according to 40 years of available REW data (Fig. 4 in the Appendices). We also compiled Ψ_{md} data from the literature (Stahl et al. 2010) recorded for the same species (n = 11) at the same site during a strong-intensity (henceforth denoted "severe") dry season in early November 2008 (REW = 0.10; Fig. 4 in the Appendices; VPD = 1.51 kPa), the second driest in the past 40 years at our site. This allowed us to compare our data with those from more severe soil drought conditions.

2.5 Hydraulic safety margins

Xylem hydraulic safety margins (HSM; MPa) were calculated as the difference between either (i) dry season midday leaf water potential ($HSM_{\Psi md\text{-}\Psi x}$; Meinzer et al. 2009) or (ii) leaf turgor loss point ($HSM_{\pi tlp\text{-}\Psi x}$; Martin-StPaul et al. 2017) and the xylem pressure inducing either 12, 50, or 88% loss of branch hydraulic conductivity. Leaf safety margins were calculated as the difference between Ψ_{md} and π_{tlp} (SM_{leaf}; MPa). All safety margins were calculated for individual trees and then averaged at the species level. We report $HSM_{\Psi md\text{-}\Psi x}$ calculated from Ψ_{md} datasets recorded both in 2018 (normal dry season; Table 1) and in 2008 (severe dry season; Table 8 in the Appendices).

2.6 Data analysis

We used ANOVA tests to estimate differences in mean species values for embolism resistance parameters, leaf water potentials and HSM, and unpaired t tests for differences in mean Ψ_{50} values between our study and other biomes. Linear models were performed to analyze trait correlations. We used a sensitivity analysis to assess the relative contributions of Ψ_{50}, Ψ_{md}, or π_{tlp} in driving the variations in HSM. To test whether species ranking in Ψ_{md} between 2018 and 2008 was conserved, we computed Kendall's coefficient of concordance (τ). The above-mentioned analyses were performed for all species with at least three individuals measured concurrently. Species that did not meet this criterion were simply projected onto the figures. All statistical analyses were performed with the R software.

3 Results

Vulnerability curves yielded embolism resistance parameters that varied strongly along a continuum across the studied species: Ψ_{12} varied from − 0.99 to − 6.78 MPa, Ψ_{50} varied from − 1.86 to − 7.63 MPa, Ψ_{88} varied from − 2.55 to − 10.22 MPa ($F > 9$; $p < 0.001$; Fig. 1, Table 1; Table 5, Fig. 5 and Fig. 6 in the Appendices) and a_x varied from 21 to 240 %MPa^{-1} (Table 5 in the Appendices). Mean community branch Ψ_{50} (− 3.93 ± 0.31 MPa; Fig. 1 and Table 1) was more negative than the worldwide mean for both tropical rainforests (− 1.70 MPa; $p < 0.001$) and tropical dry forests (− 2.40 MPa; $p < 0.001$); indeed, it was comparable to values found for drier biomes such as temperate (− 3.86 MPa; $p = 0.85$) and Mediterranean/dry forests (− 3.88 MPa; $p = 0.93$; see insert in Fig. 1; Choat et al. 2012). Leaf turgor loss point ranged from − 1.32 to − 2.15 MPa with a significant species effect ($F = 12.1$; $p < 0.001$; Table 1). Midday leaf water potential (Ψ_{md}) measured during the 2018 dry season ranged from − 0.88 to − 2.25 MPa with a significant species effect ($F = 2.4$; $p = 0.002$; Table 1).

We observed no relationship between Ψ_{50} and Ψ_{md} in 2018 (Fig. 2a), nor did we find any significant relationship between π_{tlp} and Ψ_{50} ($R^2 = 0.17$; $p = 0.09$; Fig. 2b). Indeed, π_{tlp} was relatively constant with a relatively small range (0.8 MPa) regardless of species branch xylem vulnerability to embolism along the full range of Ψ_{50} (5.8 MPa). π_{tlp} reached a plateau at ca − 2.12 MPa (i.e., the lowest 99th percentile for π_{tlp}; dotted line in Fig. 2b). However, there were significant relationships between Ψ_{12}, Ψ_{50}, and Ψ_{88}. A sensitivity analysis showed that Ψ_{50} explained as much as 88% of the variance in $HSM_{\Psi md\text{-}\Psi 50}$ and even 98% of the variance in $HSM_{\pi tlp\text{-}\Psi 50}$, with lower interspecific variation in Ψ_{md} and π_{tlp} than in Ψ_{50} (Fig. 2a,b). Species with lower π_{tlp} also had lower Ψ_{md} ($R^2 = 0.16$; $p = 0.048$; Fig. 2c). There was no other relationship between π_{tlp} and other independent hydraulic traits (Table 2). All correlations among traits are summarized in Table 2.

We found considerable interspecific variation along a continuum for xylem hydraulic safety margins. $HSM_{\Psi md\text{-}\Psi 12}$ varied from − 0.63 to 5.88 MPa ($F = 9.0$; $p < 0.001$; Table 6 in the Appendices), $HSM_{\Psi md\text{-}\Psi 50}$ varied from 0.33 to 6.73 MPa (F =

Table 1 Key branch and leaf hydraulic traits. Water potential at 50% loss of branch hydraulic conductivity (Ψ_{50}; MPa), midday leaf water potential during a normal-intensity dry season (Ψ_{md}; MPa), leaf water potential at turgor loss point (π_{tlp}; MPa), xylem hydraulic safety margins (HSM; MPa), and leaf safety margin (SM_{leaf}; MPa) derived from leaf and branch hydraulic traits for the 30 canopy-tree species sampled in French Guiana. The results of a one-way ANOVA test for species effect for each studied trait are shown. Mean ± SE, *F*, and *p* values of species comparison are displayed. Only species with at least three measured individuals are included in the analysis. Correspondance between species' code and botanical name can be found in Table 3.

Code	Ψ_{50}	Ψ_{md}	π_{tlp}	$HSM_{\Psi md-\Psi 50}$	$HSM_{\pi tlp-\Psi 50}$	SM_{leaf}
Bp	− 4.29 ± 0.23	− 1.74 ± 0.28	− 1.82 ± 0.05	2.65 ± 0.54	2.51 ± 0.28	0.10 ± 0.31
Csch	− 2.43 ± 0.28	− 1.16 ± 0.09	− 1.54 ± 0.05	1.29 ± 0.34	0.82 ± 0.29	0.44 ± 0.08
Cpri	-	− 1.37 ± 0.18	− 2.15 ± 0.12	-	-	0.78 ± 0.24
Csan	− 4.05 ± 0.04	− 1.60 ± 0.24	− 1.80 ± 0.05	2.45 ± 0.24	2.27 ± 0.05	0.18 ± 0.24
Dg	− 2.38 ± 0.13	− 1.36 ± 0.15	− 1.32 ± 0.05	1.03 ± 0.31	1.09 ± 0.17	− 0.01 ± 0.17
Ef	− 3.86 ± 0.55	− 1.29 ± 0.16	− 1.68 ± 0.05	2.53 ± 0.59	2.02 ± 0.71	0.30 ± 0.21
Eg	− 6.14 ± 0.11	− 1.29 ± 0.22	− 1.93 ± 0.05	4.86 ± 0.31	4.21 ± 0.10	0.65 ± 0.30
Ec	− 3.27	− 0.94	− 1.57	2.33	1.70	0.63
Es	− 2.88 ± 0.12	− 1.23 ± 0.17	− 1.52 ± 0.05	1.65 ± 0.19	1.29 ± 0.13	0.47 ± 0.20
Gg	− 4.99 ± 0.34	− 1.04 ± 0.22	− 1.92 ± 0.11	3.96 ± 0.24	3.05 ± 0.40	0.91 ± 0.29
Gh	− 7.63 ± 0.14	− 0.90 ± 0.11	− 1.98 ± 0.08	6.73 ± 0.10	5.64 ± 0.03	1.10 ± 0.11
Is	− 3.69	− 1.63 ± 0.17	− 1.54 ± 0.03	-	2.11	− 0.10 ± 0.22
Lper	− 3.58 ± 0.36	− 1.38 ± 0.23	− 1.82 ± 0.07	2.30 ± 0.28	1.77 ± 0.28	0.46 ± 0.17
Lpoi	− 2.14 ± 0.31	− 1.82 ± 0.07	− 2.14 ± 0.12	0.33 ± 0.32	− 0.09 ± 0.36	0.42 ± 0.07
La	-	− 1.28 ± 0.11	− 1.69 ± 0.03	-	-	0.41 ± 0.10
Lh	-	− 1.12 ± 0.24	− 1.45 ± 0.06	-	-	0.33 ± 0.25
Lm	− 2.97 ± 0.32	− 1.65 ± 0.24	− 1.76 ± 0.05	1.31 ± 0.43	1.18 ± 0.27	0.13 ± 0.23
Mb	− 6.87 ± 0.62	− 1.86 ± 0.25	− 2.07 ± 0.04	5.38 ± 0.58	4.75 ± 0.62	0.22 ± 0.18
Mc	− 2.97	− 1.69 ± 0.16	− 1.66 ± 0.02	1.44	1.29	− 0.03 ± 0.18
Pc	− 6.25 ± 0.51	− 2.25 ± 0.27	− 1.72 ± 0.05	3.19 ± 0.49	4.49 ± 0.48	− 0.58 ± 0.27
Po	− 2.41 ± 0.15	− 2.01 ± 0.55	− 1.98 ± 0.08	0.40 ± 0.66	0.35 ± 0.26	0.05 ± 0.50
Psag	− 4.94	-	-	-	-	-
Psub	− 2.93	− 1.93 ± 0.08	− 2.08 ± 0.06	0.96	0.71	0.15 ± 0.12
Qr	− 1.86 ± 0.18	− 1.23 ± 0.39	-	0.46 ± 0.42	-	-
Rs	− 4.13	− 1.61 ± 0.48	− 1.70 ± 0.12	1.64	2.19	0.02 ± 0.33
Sr	-	− 1.30 ± 0.14	− 1.49 ± 0.07	-	-	0.14 ± 0.19
Sg	− 2.09 ± 0.12	− 1.15 ± 0.08	− 1.58 ± 0.02	1.00 ± 0.08	0.50 ± 0.12	0.43 ± 0.09
Tm	− 4.13 ± 0.17	− 1.82 ± 0.29	− 1.75 ± 0.04	2.31 ± 0.32	2.39 ± 0.18	− 0.08 ± 0.26
Vm	− 5.27 ± 0.30	− 0.88 ± 0.19	− 1.62 ± 0.03	4.38 ± 0.40	3.64 ± 0.31	0.74 ± 0.17
Va	-	− 1.90 ± 0.16	− 1.94 ± 0.05	-	-	0.05 ± 0.17
All	*− 3.93 ± 0.31*	*− 1.46 ± 0.07*	*− 1.75 ± 0.04*	*2.37 ± 0.35*	*2.17 ± 0.32*	*0.30 ± 0.01*
F	*28.0*	*2.4*	*12.1*	*19.4*	*22.6*	*1.9*
p	*< 0.001*	*0.002*	*< 0.001*	*< 0.001*	*< 0.001*	*0.02*

19.4; $p < 0.001$; Table 1), and $HSM_{\Psi md-\Psi 88}$ varied from 1.08 to 8.34 MPa ($F = 19.6$; $p < 0.001$; Table 6 in the Appendices). As much as 78% of the species investigated in 2018 exhibited more negative Ψ_{12} than Ψ_{md} values and therefore had a positive $HSM_{\Psi md-\Psi 12}$ with an average of 1.28 ± 0.33 MPa. All species had more negative Ψ_{50} and Ψ_{88} than Ψ_{md} values, and $HSM_{\Psi md-\Psi 50}$ and $HSM_{\Psi md-\Psi 88}$ remained positive for all species with an average of 2.37 ± 0.35 MPa and 3.46 ± 0.42, respectively (Fig. 2a, Tables 1, Tables 5 and 6 in the Appendices). $HSM_{\pi tlp-\Psi 12}$ varied from − 1.05 to 4.79 MPa ($F = 7.3$; $p < 0.001$; Table 6 in the Appendices), $HSM_{\pi tlp-\Psi 50}$ varied from − 0.09 to 5.64 MPa ($F = 22.6$; $p < 0.001$; Table 1), and $HSM_{\pi tlp-\Psi 88}$ varied from 0.87 to 8.10 MPa ($F = 27.8$; $p < 0.001$; Table 6 in the Appendices). As much as 74% of the species exhibited a positive $HSM_{\pi tlp-\Psi 12}$, with an average of 1.03 ± 0.30 MPa (Table 6 in the Appendices). All species but one (*Lecythis poiteaui*) had more negative Ψ_{50} than π_{tlp} values and therefore had a positive $HSM_{\pi tlp-\Psi 50}$, with an average of 2.17 ± 0.32 MPa (Fig. 2b and Table 1). All species had a positive $HSM_{\pi tlp-\Psi 88}$ with an average of 3.31 ± 0.39 MPa. The relationship between π_{tlp} and Ψ_{50} thus restricted species to the area bound by the lower limit of π_{tlp} and the 1:1 line between the two considered traits.

There was a significant species effect in SM_{leaf} measured in 2018 ($F = 1.9$; $p = 0.02$; Table 1). π_{tlp} values were more negative than Ψ_{md} values measured in 2018 for more than 80% of the species (Fig. 2c), with subsequent positive SM_{leaf} ranging from − 0.58 to 1.10 MPa with an average of 0.30 ± 0.01 MPa (Table 1).

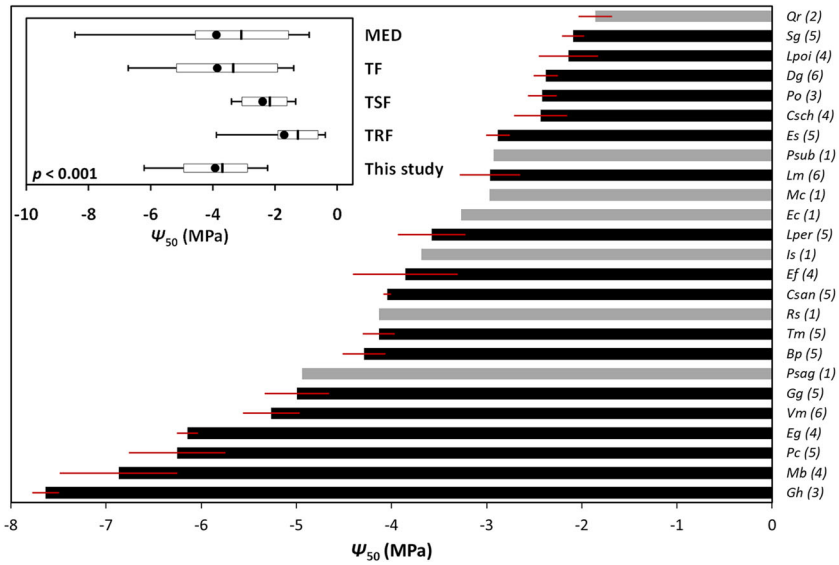

Fig. 1 Water potential at 50% loss of branch hydraulic conductivity (Ψ_{50}; MPa) for the 25 canopy-tree species sampled in French Guiana. Each bar represents species mean (black, $n \geq 3$; gray $n < 3$) with the number of replicates per species indicated in parentheses. Error bars represent standard errors of the mean. Insert: box plots of mean Ψ_{50} values for 329 adult tree species from different biomes (MED: Mediterranean forests/Woodlands, n = 77; TF: Temperate Forest, n = 133; TSF: Tropical Seasonal Forest, n = 54; TRF: Tropical Rainforest, n = 65) extracted from the meta-analysis by Choat et al. (2012) and with data for the 25 species in this study. Boxes show the mean (black dots), median (horizontal bar), 25th and 75th percentiles; error bars show the 10th and 90th percentiles

Species Ψ_{md} recorded during the 2008 severe dry season ranged from − 1.57 to − 3.03 MPa (Table 8 in the Appendices; Stahl et al. 2010), showed strong interspecific variation (F = 18; p < 0.001), and was, on average, 0.62 ± 0.10 MPa (57%) more negative than Ψ_{md} in 2018 for the species in common to both years (p < 0.001; data not shown). Consequently, the $HSM_{\Psi md\text{-}\Psi 50}$ calculated from the Ψ_{md} measured in 2008 for ten species was lower

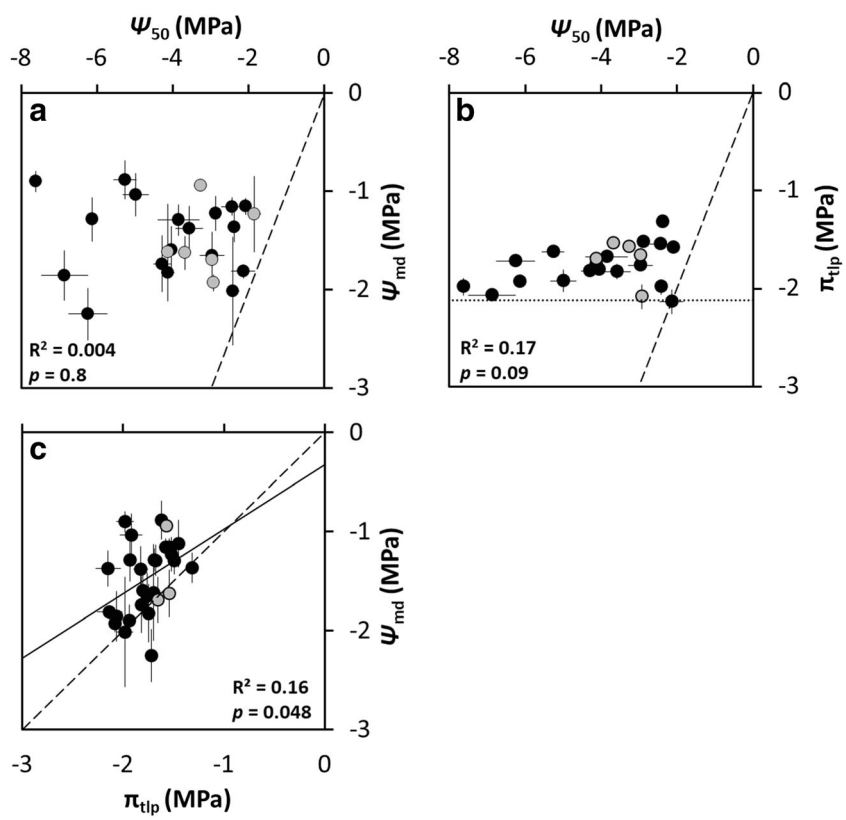

Fig. 2 Relationships between Ψ_{50}, the water potential at 50% loss of branch hydraulic conductivity (Ψ_{50}; MPa), and **a** dry season midday leaf water potential (Ψ_{md}; MPa), **b** the water potential at turgor loss point (π_{tlp}; MPa), and **c** π_{tlp} and Ψ_{md}, for the 30 canopy-tree species sampled in French Guiana (black $n \geq 3$; gray $n < 3$). All error bars represent standard errors of the mean. The 1:1 line (dashed line) is represented in all panels; the 99% percentile of π_{tlp} (− 2.12 MPa; dotted line) is represented in **b**; and the regression (solid line) is represented in **c**. Coefficients of determination (R^2) and significance levels (p) are shown

Table 2 Pearson's correlation coefficients (r) between hydraulic traits and species bioclimatic affiliation for the canopy-tree species sampled in French Guiana. Bivariate comparisons were applied using species means for each variable, with n varying from 18 to 26 species. r values are shown in bold type when significant ($p < 0.05$). Abbreviations are as follows: a_x (MPa^{-1}) represents the slope of the vulnerability curve; Ψ_{12}, Ψ_{50}, and Ψ_{88} (MPa) represent the water potential at 12, 50, and 88% of branch embolism, respectively; Ψ_{md} (MPa) represents midday leaf water potential measured in 2018; π_{tlp} (MPa) represents leaf turgor loss point; $HSM_{\Psi md\text{-}\Psi 50}$ and $HSM_{\pi tlp\text{-}\Psi 50}$ (MPa) represent the hydraulic safety margins calculated as the difference between Ψ_{md} or πtlp and Ψ_{50}; SMleaf represents the leaf safety margin calculated as the difference between Ψ_{md} and π_{tlp}

	a_x	Ψ_{12}	Ψ_{50}	Ψ_{88}	Ψ_{md}	π_{tlp}	HSMΨmd-Ψ50	HSMπtlp-Ψ50	SM_{leaf}
a_x	-	0.07	0.25	0.46	0.11	0.09	− 0.23	− 0.25	− 0.12
Ψ_{12}	-	-	*0.92*	*0.77*	− 0.18	0.33	*− 0.90*	*− 0.92*	− 0.31
Ψ_{50}	-	-	-	*0.96*	− 0.06	0.41	*− 0.96*	*− 0.99*	− 0.22
Ψ_{88}	-	-	-	-	0.03	0.43	*− 0.91*	*− 0.95*	− 0.14
Ψ_{md}	-	-	-	-	-	*0.40*	0.32	0.11	*0.79*
π_{tlp}	-	-	-	-	-	-	− 0.35	− 0.29	− 0.23
HSMΨmd-Ψ50	-	-	-	-	-	-	-	*0.96*	0.46
HSMπtlp-Ψ50	-	-	-	-	-	-	-	-	0.20
SM_{leaf}	-	-	-	-	-	-	-	-	-

than in 2018 though it remained positive, ranging from 0.52 to 2.39 MPa with an average of 1.43 MPa ± 0.22 (Figs. 3b; Fig. 7 and Table 8 in the Appendices). Mean SM_{leaf} calculated from Ψ_{md} measured in 2008 for 12 species ranged from − 1.09 to 0.01 MPa, with an average of − 0.43 ± 0.09 MPa. SM_{leaf} was negative for all species but one (*Symphonia sp. 1*; Fig. 3a and Table 8 in the Appendices) and species ranking in SM_{leaf} was not conserved between years (τ = 0.5; ns; Fig. 3a).

4 Discussion

Considerable interspecific variability in branch xylem vulnerability to embolism In this study, our sampling of 25 tropical rainforest canopy-tree species showed a four-fold range of magnitude in branch xylem vulnerability to embolism (Fig. 1, Table 1). This range encompasses 72% of the previously observed angiosperm variation in Ψ_{50} at the global scale (Choat et al. 2012) and expands the range of known branch xylem vulnerability to embolism for tropical forest Angiosperm tree species (Choat et al. 2012; Nolf et al. 2015; Rowland et al. 2015; Christoffersen et al. 2016; Powell et al. 2017; Santiago et al. 2018). The limited importance of confounding factors (e.g., genetics, ontogeny, competition, habitat) indicates that the observed interspecific variability was mostly related to the species' intrinsic functional characteristics.

Mean community branch Ψ_{50} (− 3.93 ± 0.31 MPa; Fig. 1 and Table 1) was much more negative than the worldwide mean for tropical rainforests; it was also more negative than the mean values published to date for *terra firme* canopy-tree species (− 2.31 ± 0.20 MPa; Sperry et al. 1988; Machado and Tyree 1994; Tyree et al. 1998; Choat et al. 2007; Sperry et al. 2007; Meinzer et al. 2008; Nolf et al. 2015; Rowland et al. 2015; Powell et al. 2017; Santiago et al. 2018) and was comparable to values found for drier biomes (Fig. 1). Our results therefore clearly contrast with the global and inter-biome pattern of interspecific variation in branch embolism resistance, where total precipitation is thought to be the main driver (Maherali et al. 2004; Choat et al. 2012).

The differences in branch xylem vulnerability to embolism between our study and the existing literature on tropical rainforests could be due to differences in water availability or habitat type, the species' ontogenetic stage of development, species phylogeny or methodological aspects of hydraulic measurements. However, the lower branch xylem vulnerability to embolism we found cannot be explained by differences in water availability since all our measurements were conducted on similar habitats (i.e., *terra firme*). Furthermore, the differences are unlikely to be due to either ontogeny or limited phylogenetic differences since we sampled branches of mature canopy trees covering a broad range of species and botanical families, as was also the case for the previously recorded Ψ_{50} values. It therefore appears that methodological choices are probably the main reason for the inconsistencies that have appeared across studies. The precautions we took when sampling, combined with the use of the in situ flow-centrifuge technique, makes it unlikely that our measurements were affected by native embolism. Herein, we therefore provide robust results for an ecosystem where the scarcity of data limits our understanding of the hydraulic functioning and fate of tree species (Cochard and Delzon 2013; Delzon and Cochard 2014). Although it has been shown that branch xylem vulnerability to embolism varies along macro- (Maherali et al. 2004; Choat et al. 2012) and micro-environmental scales of water availability (Oliveira et al. 2019), we still must decipher the past and present ecological processes underlying the large

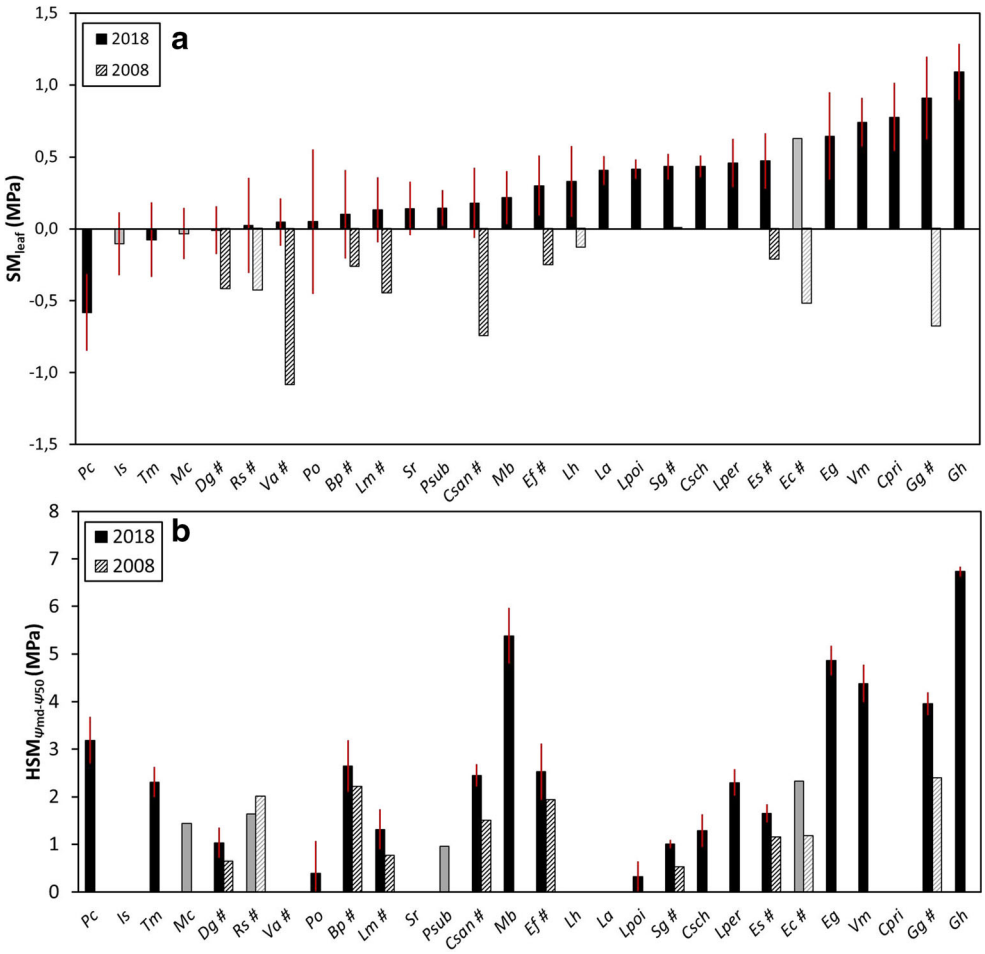

Fig. 3 Leaf safety margin (SM_{leaf}; MPa) and xylem safety margin ($HSM_{\Psi md\text{-}\Psi 50}$; MPa) during a normal (2018) and a severe (2008) dry season. **a** SM_{leaf} was calculated as the difference between dry season midday leaf water potential (Ψ_{md}) and the water potential at turgor loss point (π_{tlp}; MPa) for, respectively, 28 and 12 canopy-tree species sampled in French Guiana. Species common to both years are identified by hash signs (#). **b** $HSM_{\Psi md\text{-}\Psi 50}$ was calculated as the difference between Ψ_{md} and the water potential at 50% loss of branch hydraulic conductivity (Ψ_{50}; MPa) for, respectively, 23 and 12 canopy-tree species sampled in French Guiana. The ranking of species between both years was not retained for SM_{leaf} ($\tau = 0.5$; $n = 8$; ns) but was retained for $HSM_{\Psi md\text{-}\Psi 50}$ ($\tau = 0.71$; $p < 0.01$). Each bar represents the species mean for 2018 (black; $n \geq 3$; gray, $n < 3$) and 2008 (black dashes, $n > 3$; gray dashes, $n < 3$) and all error bars represent standard errors of the mean for SM_{leaf} measured in 2018

interspecific variability we found in co-occurring rainforest species in the same habitat. Several approaches may be pertinent, for example, the investigation of trade-offs related to hydraulic safety vs efficiency (Santiago et al. 2018), the existence of contrasting strategies of drought resistance (Pivovaroff et al. 2016), or better knowledge of species biogeographic distribution in relation to water availability (Esquivel-Muelbert et al. 2019).

Low risk of hydraulic failure during a normal dry season Our results show that most of the studied species share a low risk of hydraulic failure during a normal dry season since both xylem hydraulic safety margins were large with regard to critical thresholds of branch embolism (i.e., Ψ_{50} and Ψ_{88}). One of our major findings concerns leaf turgor loss point, for which we gathered one of the largest datasets to date for tropical rainforest tree species. The range of π_{tlp} we found confirms previous findings (Marechaux et al. 2015) while the mean was more negative than what is currently generally accepted for tropical rainforests (Bartlett et al. 2012a, b, 2016; Zhu et al. 2018). However, π_{tlp} was relatively constant along the full range of Ψ_{50}. Our results suggest that turgor loss, which was used in this study as a proxy for stomatal closure, precedes the rapid spread of branch embolism (Brodribb et al. 2003; Creek et al. 2018), regardless of species branch xylem vulnerability to embolism. This result both supports (Mencuccini et al. 2015; Martin-StPaul et al. 2017) and contradicts (Christoffersen et al. 2016) patterns found in recent global meta-analyses, and it is consistent with the rather conservative behavior of rainforest species with regard to water-use (Fisher et al. 2006).

Although we found that higher leaf tolerance to desiccation allows leaves to function at more negative water potentials during the dry season (Fig. 2c; Zhu et al. 2018), our results indicate that in this ecosystem, Ψ_{50} and π_{tlp} are not linearly coupled to ensure the maintenance of leaf functioning. Therefore, lower branch xylem vulnerability to embolism may not involve maintaining gaseous exchanges to maximize carbon gain as long as possible during drought (Jones and Sutherland 1991), but rather maintaining tissue water potential (Martin-StPaul et al. 2017). This indicates that preserving perennial organs (i.e., branches) is usually favored at the expense of cheaper, renewable organs (i.e., leaves). However, the six species that would reach Ψ_{12} before π_{tlp} may be able to tolerate a certain percentage of branch hydraulic conductivity loss or this may indicate that other mechanisms are acting (e.g., at the leaf level) to avoid the initial spread of branch embolism. In order to have a more comprehensive understanding of how the functioning of branches and leaves interact, we need to

investigate leaf drought resistance in greater depth, notably to evaluate the potential role of the loss of leaf conductance prior to turgor loss (i.e., the loss of leaf extra-xilary hydraulic conductance; Scoffoni et al. 2017), hydraulic segmentation (Pivovaroff et al. 2014), vulnerability segmentation (Zhu et al. 2016), and cuticular conductance (Duursma et al. 2019) as potentially determinant drought-resistance features in rainforest tree species.

During our study, we also evaluated whether species exceeded xylem hydraulic safety margins ($HSM_{\Psi md\text{-}\Psi 50}$) during a normal dry season. Our results show that most of the studied species operate without developing any xylem embolism. Only five showed slightly negative $HSM_{\Psi md\text{-}\Psi 12}$ meaning that branches could have been subjected to some degree of embolism. However, all remained above Ψ_{50} (Fig. 2 and Table 1) and far from Ψ_{88} (> 1 MPa), the threshold water potential thought to cause irreversible hydraulic failure in angiosperms (Table 6 in the Appendices; Urli et al. 2013). However, six species had relatively narrow values of $HSM_{\Psi md\text{-}\Psi 50}$, close to or lower than 1 MPa. Overall, our data support the view that the hydraulic safety margins of most tropical rainforest tree species are wide during a normal dry season (Delzon and Cochard 2014).

Limited risk of hydraulic failure during a severe dry season In 2008, our site experienced the second most severe dry season in the past four decades (Aguilos et al. 2019). The SM_{leaf} values estimated in 2008 were equal to or below zero, indicating that most species had their stomata closed (Fig. 3a and Table 8 in the Appendices). Additional water loss and the resulting decline in water potential from π_{tlp} to Ψ_{md} in 2008 could therefore have been due to cuticular transpiration (Martin-StPaul et al. 2017; Choat et al. 2018; Duursma et al. 2019). In these conditions, water potential gradients between branches and leaves are strongly reduced and midday leaf water potential measured that year can therefore be considered as an estimate of the lowest branch water potential these trees may have experienced in the past four decades (i.e., minimum water potential). However, the same year, though there was a clear decrease in photosynthetic assimilation for most of the trees, it was never null, some trees were not affected (Stahl et al. 2013), no leaf mortality was observed (Clément Stahl, personal communication), and litterfall was similar to other dry seasons (Wagner et al. 2013). Despite considerable diversity of response to drought, this suggests that no leaves were fully embolized.

Additionally, we found no clear pattern in species SM_{leaf} between a normal and a severe dry season (Fig. 3a), indicating that the response to drought might be non-linear and affected by threshold effects depending on the intensity and duration of the dry season. The lack of a clear pattern could also arise from the large uncertainties involved or the low sample size for some of the measured species. For the ten species in common to both years, the calculated $HSM_{\Psi md\text{-}\Psi 50}$ was narrower in 2008 than in 2018, but always remained positive (Figs. 3b; Fig. 7 and Table 8 in the Appendices). Unfortunately, Ψ_{md} and therefore $HSM_{\Psi md\text{-}\Psi 50}$ were not available in 2008 for some species with the narrowest $HSM_{\Psi md\text{-}\Psi 50}$ in 2018. Yet, species' ranking was comparable between the 2 years ($\tau = 0.71$; $p < 0.01$; data not shown), hinting that some species with relatively narrow $HSM_{\Psi md\text{-}\Psi 50}$ in 2018 could have suffered from reduced branch hydraulic conductivity during the severe 2008 dry season due to partial branch xylem embolism. However, this was not a general rule since our data support that most canopy tree species, which experience steep gradients in evaporative demand even during the rainy season, develop an embolism resistant xylem, and share a limited risk of hydraulic failure during a severe dry season. Such severe dry season droughts due to anthropogenic-induced climate change are projected to increase over the next century in the Eastern-Amazon (Duffy et al. 2015). Though it is believed that previous shifts in species composition occurred throughout the late Pleistocene and Holocene because of dramatic changes in climate and in rainfall seasonality (Bonal et al. 2016), a vast majority of the Amazon basin remained as intact forest (Mayle and Power 2008). At present, there is already evidence that the recruitment of drought-tolerant taxa has increased over the past three decades in Amazonia in areas affected by droughts, while mortality among taxa affiliated to wet conditions has simultaneously increased (Esquivel-Muelbert et al. 2019). However, such changes in tree communities lag behind the pace of climate change, thus raising concern about the fate of these rainforest ecosystems. A trait-based approach encompassing a mechanistic understanding of drought resistance may help decipher what facilitates such changes in species composition and may help predict how long species will be able to avoid reaching catastrophic levels of branch embolism, which still needs to be addressed by modeling approaches.

5 Conclusions

In this study, we report key branch and leaf hydraulic traits related to drought response and resistance for a set of 30 co-occurring Neotropical rainforest canopy-tree species. We found that (i) rainforest canopy-tree species that grow with elevated mean annual precipitation and yearly experience several months of meteorological drought and reduced soil water availability can have high resistance to embolism and are more resistant than what was previously thought and that (ii) most species have a low risk of hydraulic failure and are well able to withstand normal and even severe dry seasons thanks to early leaf turgor loss and low branch xylem vulnerability to embolism. Yet, in the forest we studied, such a severe drought has not occurred in the previous four decades and it is therefore unlikely that canopy-tree species suffered from hydraulic failure during that time, even during severe dry seasons as the one experienced in 2008. Our results therefore support the idea that, at least for the most abundant canopy-tree species, expected climate change over the next decades, at least in terms of water availability, will not directly or severely affect

the survival of these species at the adult stage in *terra-firme* forests of the Guiana Shield. Yet, considering that the studied canopy trees are long-living organisms, they may have previously experienced severe droughts in the past beyond our records and will most likely do in a near future, while considerable uncertainties remain on their capacity to withstand repeated drought episodes. Whether species capacity to avoid hydraulic failure is influencing the slow compositional shift in the Amazon rainforest at the early development stage (Esquivel-Muelbert et al. 2019) in response to increasingly frequent and severe dry seasons is a worthy question. Moreover, little is known about the drought-resistance characteristics of the less-abundant species that compose the vast majority of Neotropical tree communities. We therefore encourage further research in this domain to better predict tree species' and forest communities' fate in a rapidly changing climate (Brodribb 2017).

Acknowledgments We are grateful for the technical assistance of Benoit Burban who also provided climatic data. We thank Fabien Wagner and Maricar Aguilos for providing water availability data and Déborah Corso and Gaëlle Capdeville for assistance with measuring xylem embolism resistance. We also thank the climbing team (Valentine Alt, Samuel Counil, Anthony Percevaux, and Elodie Courtois) for canopy sampling.

Funding information This study is part of the Guyaflux program, under the auspices of SOERE F-ORE-T, and is supported annually by Ecofor, Allenvi, and the French national research infrastructure, ANAEE-F (ANAEE-France: ANR-11-INBS-0001). This study was funded by the GFclim project (FEDER 20142020, Project GY0006894) and an "Investissement d'Avenir" grant from the Agence Nationale de la Recherche (CEBA: ANR-10-LABX-0025; ARBRE, ANR-11-LABX-0002-01). CZ received an assistantship from Pôle A2F, Université de Lorraine, France. AE-M was supported by the NERC TREMOR project and the ERC grants, T-Forces (291585) and TreeMort (758873). The authors have no conflict of interest.

Data availability statement All data corresponding to species' mean trait values are included in this published article (and its supplementary information files). All raw data generated during the current study are not publicly available at the moment because the authors of the study wish to keep them for further analysis. They will then be made public on an online repository. In the meantime, they can nonetheless be made available by the corresponding author on request.

Compliance with ethical standards

Conflicts of interest The authors declare that they have no conflict of interest.

Appendices

Table 3 Species full botanical name, family, species' abbreviation code, and percent of total tree basal area at our site (TBA; %) for the 30 rainforest canopy-tree species sampled in French Guiana

Species	Family	Code	TBA
Bocoa prouacensis Aubl.	Fabaceae	Bp	1.7
Chaetocarpus schomburgkianus (Kuntze)	Peraceae	Csch	0.8
Chrysophyllum prieurii A. DC.	Sapotaceae	Cpri	1.0
Chrysophyllum sanguinolentum (Pierre) Baehni	Sapotaceae	Csan	0.4
Dicorynia guianensis Amshoff	Fabaceae	Dg	2.2
Eperua falcata Aubl.	Fabaceae	Ef	15.4
Eperua grandiflora (Aubl.) Benth.	Fabaceae	Eg	4.7
Eschweilera coriacea (DC.) S.A. Mori	Lecythidaceae	Ec	0.4
Eschweilera sagotiana Miers	Lecythidaceae	Es	8.0
Goupia glabra Aubl.	Goupiaceae	Gg	1.0
Gustavia hexapetala (Aubl.) Sm.	Lecythidaceae	Gh	0.5
Iryanthera sagotiana (Benth.) Warb.	Myristicaceae	Is	0.4
Lecythis persistens Sagot	Lecythidaceae	Lper	2.3
Lecythis poiteaui O. Berg	Lecythidaceae	Lpoi	0.3
Licania alba (Bernouilli) Cuatrec.	Chrysobalanaceae	La	3.4
Licania heteromorpha Benth.	Chrysobalanaceae	Lh	1.6
Licania membranacea Sagot ex Laness.	Chrysobalanaceae	Lm	1.1
Manilkara bidentata (A. DC.) A. Chev.	Sapotaceae	Mb	0.6
Moronobea coccinea Aubl.	Clusiaceae	Mc	1.6
Pradosia cochlearia (Lecomte) T.D. Penn.	Sapotaceae	Pc	2.6
Protium opacum Swart	Burseraceae	Po	0.3
Protium sagotianum Marchand	Burseraceae	Psag	0.1
Protium subserratum (Engl.) Engl	Burseraceae	Psub	0.2
Qualea rosea Aubl.	Vochysiaceae	Qr	2.3
Recordoxylon speciosum (Benoist) Gazel	Fabaceae	Rs	1.5
Sextonia rubra (Mez) van der Werff	Lauraceae	Sr	1.1
Symphonia globulifera L.f. sp. 1	Clusiaceae	Sg	1.9
Tachigali melinonii (Harms) Zarucchi & Her.	Fabaceae	Tm	0.6
Virola michelii Heckel	Myristicaceae	Vm	0.4
Vouacapoua americana Aubl.	Fabaceae	Va	1.9

Table 4 Number of replicates for key branch and leaf hydraulic traits. Water potential at 50% loss of branch hydraulic conductivity (Ψ_{50}; MPa), midday leaf water potential during a normal intensity dry season (Ψ_{md}; MPa), leaf water potential at turgor loss point (π_{tlp}; MPa), xylem hydraulic safety margins (HSM; MPa), and leaf safety margin (SM_{leaf}; MPa) derived from leaf and branch hydraulic traits for the 30 canopy-tree species sampled in French Guiana. Results of a one-way ANOVA test for species effect for each studied trait are shown. Only species with at least three measured individuals are included in the analysis

Sp.	n Ψ_{50}	n Ψ_{md}	n π_{tlp}	n $HSM_{\Psi md-\Psi 50}$	n $HSM_{\pi tlp-\Psi 50}$	n SM_{leaf}
Bp	5	8	10	5	5	8
Csch	4	5	7	4	4	5
Cpri	-	3	3	-	-	3
Csan	5	5	6	5	5	5
Dg	6	7	10	5	6	7
Ef	4	5	5	4	3	4
Eg	4	4	7	4	4	4
Ec	1	1	1	1	1	1
Es	5	7	9	5	5	6
Gg	5	5	6	5	5	5
Gh	3	3	5	3	3	3
Is	1	2	3	-	1	2
Lper	5	6	7	5	5	6
Lpoi	4	4	6	4	4	4
La	-	3	3	-	-	3
Lh	-	3	3	-	-	3
Lm	6	6	10	6	6	6
Mb	4	4	7	3	4	4
Mc	1	2	2	1	1	2
Pc	5	6	8	3	5	6
Po	3	3	5	3	3	3
Psag	1	-	-	-	-	-
Psub	1	3	4	1	1	3
Qr	2	3	-	2	-	-
Rs	1	3	4	1	1	3
Sr	-	3	4	-	-	3
Sg	5	6	8	5	5	6
Tm	5	5	5	5	5	5
Vm	6	6	6	6	6	6
Va	-	5	5	-	-	5

Table 5 Key branch and leaf hydraulic traits. Water potential at 12 and 88% loss of branch hydraulic conductivity (Ψ_{12}, Ψ_{88}; MPa) and the slope of vulnerability curves (a_x; $\%MPa^{-1}$) for the 25 canopy-tree species sampled in French Guiana. Results of a one-way ANOVA test for species effect for each studied trait are shown. Mean ± SE, *F*, and *p* values are displayed. Only species with at least three measured individuals are included in the analyses

Code	Ψ_{12}	Ψ_{88}	a_x
Bp	− 3.35 ± 0.51	− 5.23 ± 0.26	86 ± 24
Csch	− 1.19 ± 0.29	− 3.68 ± 0.43	52 ± 13
Csan	− 3.61 ± 0.09	− 4.48 ± 0.09	144 ± 37
Dg	− 1.35 ± 0.19	− 3.41 ± 0.15	56 ± 10
Ef	− 2.83 ± 0.80	− 4.88 ± 0.58	89 ± 40
Eg	− 5.38 ± 0.32	− 6.90 ± 0.19	93 ± 30
Ec	− 3.06	− 3.48	240
Es	− 2.56 ± 0.11	− 3.21 ± 0.16	172 ± 19
Gg	− 3.40 ± 0.58	− 6.58 ± 0.22	38 ± 9
Gh	− 6.78 ± 0.62	− 8.49 ± 0.36	109 ± 49
Is	− 1.30	− 6.08	21
Lper	− 2.59 ± 0.34	− 4.56 ± 0.43	59 ± 12
Lpoi	− 1.18 ± 0.20	− 3.10 ± 0.62	98 ± 52
Lm	− 1.41 ± 0.25	− 4.53 ± 0.56	53 ± 24
Mb	− 3.52 ± 1.06	− 10.22 ± 0.69	22 ± 9
Mc	− 2.52	− 3.41	113
Pc	− 4.84 ± 0.95	− 7.67 ± 0.17	68 ± 21
Po	− 1.73 ± 0.31	− 3.10 ± 0.20	100 ± 44
Psag	− 4.58	− 5.30	139
Psub	− 1.44	− 4.41	34
Qr	− 0.99 ± 0.39	− 2.72 ± 0.04	62 ± 15
Rs	− 2.95	− 5.32	42
Sg	− 1.64 ± 0.21	− 2.55 ± 0.04	132 ± 25
Tm	− 2.61 ± 0.41	− 5.66 ± 0.40	44 ± 12
Vm	− 3.83 ± 0.59	− 6.70 ± 0.18	45 ± 9
All	**− 2.83 ± 0.29**	**− 5.03 ± 0.39**	**84 ± 10**
F	**8.3**	**31.8**	**2.7**
p	**< 0.001**	**< 0.001**	**0.002**

Table 6 Xylem hydraulic safety margins (HSM, MPa) derived from leaf and branch hydraulic traits for the 25 canopy-tree species sampled in French Guiana. Results of a one-way ANOVA test for species effect for each studied trait are shown. Mean ± SE, *F*, and *p* values are displayed. Only species with at least three measured individuals are included in the analyses

Code	$HSM_{\Psi md-\Psi 12}$	$HSM_{\Psi md-\Psi 88}$	$HSM_{\pi tlp-\Psi 12}$	$HSM_{\pi tlp-\Psi 88}$
Bp	1.70 ± 0.85	3.59 ± 0.28	1.57 ± 0.55	3.45 ± 0.29
Csch	0.04 ± 0.39	2.53 ± 0.43	− 0.43 ± 0.32	2.06 ± 0.41
Csan	2.02 ± 0.2	2.89 ± 0.29	1.84 ± 0.13	2.70 ± 0.06
Dg	0.38	2.07 ± 0.30	0.05 ± 0.23	2.12 ± 0.18
Ef	1.51 ± 0.73	3.55 ± 0.72	1.00 ± 1.10	3.05 ± 0.73
Eg	4.10 ± 0.44	5.62 ± 0.33	3.45 ± 0.33	4.97 ± 0.16
Ec	2.12	2.54	1.49	1.91
Es	1.32 ± 0.14	1.97 ± 0.24	0.97 ± 0.13	1.62 ± 0.14
Gg	2.37 ± 0.42	5.55 ± 0.31	1.46 ± 0.65	4.64 ± 0.23
Gh	5.88 ± 0.53	7.59 ± 0.46	4.79 ± 0.52	6.49 ± 0.46
Is	-	-	− 0.28	4.50
Lper	1.31 ± 0.33	3.28 ± 0.32	0.78 ± 0.29	2.75 ± 0.34
Lpoi	− 0.63 ± 0.15	1.29 ± 0.64	− 1.05 ± 0.21	0.87 ± 0.67
Lm	− 0.25 ± 0.34	2.87 ± 0.65	− 0.38 ± 0.25	2.74 ± 0.5
Mb	2.42 ± 1.07	8.34 ± 0.78	1.40 ± 1.08	8.10 ± 0.67
Mc	0.99	1.88	0.85	1.74
Pc	1.12 ± 0.9	5.26 ± 0.12	3.08 ± 0.93	5.91 ± 0.15
Po	− 0.28 ± 0.86	1.08 ± 0.48	− 0.33 ± 0.39	1.03 ± 0.26
Psag	-	-	-	-
Psub	− 0.53	2.44	− 0.78	2.20
Qr	− 0.41 ± 0.21	1.32 ± 0.64	-	-
Rs	0.45	2.82	1.01	3.38
Sg	0.55 ± 0.18	1.46 ± 0.05	0.04 ± 0.22	0.95 ± 0.03
Tm	0.79 ± 0.43	3.83 ± 0.53	0.87 ± 0.39	3.91 ± 0.42
Vm	2.95 ± 0.62	5.81 ± 0.35	2.21 ± 0.59	5.07 ± 0.20
All	**1.28 ± 0.33**	**3.46 ± 0.42**	**1.03 ± 0.30**	**3.31 ± 0.39**
F	**9.0**	**19.6**	**7.3**	**27.8**
p	**< 0.001**	**< 0.001**	**< 0.001**	**< 0.001**

Table 7 Presence of exudates, mean values, and standard error (SE) of maximum vessel length (MVL, cm) and branch diameter calculated as the average diameter at both ends (mm; including bark) as well as the number of individual replicates for 25 canopy-tree species sampled in French Guiana. Species with MVL > 100 cm were excluded from the sample for measurements of branch resistance to embolism, with the exception of *Eperua falcata*, *Goupia glabra*, and *Licania membranacea* for which we sampled smaller diameter branches, since branch diameter and MVL were positively related (Jacobsen et al. 2012; this study). Results of a one-way ANOVA test for species effect for each studied trait are shown. Mean ± SE, *F*, and *P* values are displayed. Only species with at least three measured individuals are included in the analyses

Species	Exudates	MVL	Diameter	*n*
Bp	-	61.3 ± 1.5	15.3 ± 0.4	6
Csch	-	42.1 ± 2.5	14.3 ± 0.4	10
Csan	Yes	24.1 ± 2.1	15.4 ± 0.7	9
Dg	-	60.0 ± 3.5	15.9 ± 0.6	10
Ef	-	140.5 ± 3.5	19.4 ± 0.6	7
Eg	-	92.8 ± 2.6	17.6 ± 0.7	9
Ec	-	30.0	14.8	1
Es	-	29.4 ± 1.5	14.2 ± 0.9	7
Gg	-	111.5 ± 3.4	16.3 ± 0.8	7
Gh	-	40.1 ± 1.8	14.1 ± 0.5	6
Is	Yes	57.0	15.6	1
Lper	-	49.2 ± 1.7	14.0 ± 0.4	5
Lpoi	-	52.3 ± 3.6	14.3 ± 0.5	8
Lm	-	111.0 ± 3.4	15.9 ± 0.6	13
Mb	Yes	72.6 ± 4.3	16.0 ± 0.6	9
Mc	Yes	71.0	13.6	1
Pc	Yes	44.9 ± 2.0	14.0 ± 0.4	10
Po	-	51.7 ± 1.9	13.9 ± 0.3	5
Psub	-	54.8 ± 3.7	15 ± 0.5	4
Qr	-	49.4 ± 2.2	15.5 ± 0.7	7
Rs	-	93.2 ± 1.7	17.2 ± 0.6	5
Sg	Yes	67.7 ± 3.3	13.4 ± 0.4	5
Tm	-	75.7 ± 3.1	17.3 ± 0.4	5
Vm	Yes	39.6 ± 2.1	14.5 ± 0.7	6
All		**62.2 ± 5.8**	**15.3 ± 0.3**	-
***F* test**		**10.6**	**2.8**	-
***p* value**		**< 0.001**	**< 0.001**	-

Table 8 Mean values and standard error (SE) of midday leaf water potential (Ψ_{md}; MPa) measured during the severe 2008 dry season (Ψ_{md}; MPa; Stahl et al. 2010), the driest in the past decade (Aguilos et al. 2019), and the second driest in the past four decades. Results are shown for the 12 canopy-tree species sampled at the same site in French Guiana in 2008 that are common to our study. Xylem hydraulic safety margins computed from embolism resistance traits ($HSM_{\Psi md-\Psi x}$) or leaf safety margins computed from leaf turgor loss point measured in 2018 (SM_{leaf}) are also shown

Species	n Ψ_{md}	Ψ_{md}	$HSM_{\Psi md-\Psi 12}$	$HSM_{\Psi md-\Psi 50}$	SM_{leaf}
Bp	3	− 2.08 ± 0.26	1.27	2.21	− 0.26
Csan	5	− 2.55 ± 0.18	1.06	1.50	− 0.75
Dg	4	− 1.74 ± 0.09	− 0.39	0.64	− 0.42
Ef	5	− 1.93 ± 0.14	0.90	1.93	− 0.25
Ec	4	− 2.09 ± 0.12	0.97	1.18	− 0.52
Es	4	− 1.74 ± 0.04	0.82	1.14	− 0.22
Gg	1	− 2.60	0.80	2.39	− 0.68
Lh	2	− 1.58 ± 0.33	-	-	-0.13
Lm	5	− 2.21 ± 0.12	− 0.80	0.76	− 0.45
Rs	2	− 2.13 ± 0.02	0.82	2.01	− 0.43
Sg	5	− 1.57 ± 0.12	0.07	0.52	0.01
Va	10	− 3.03 ± 0.08	-	-	− 1.09
All	**-**	**− 2.10 ± 0.13**	**0.55 ± 0.22**	**1.43 ± 0.22**	**− 0.43 ± 0.09**
F	**-**	**18**	**-**	**-**	**-**
p	**-**	**< 0.001**	**-**	**-**	**-**

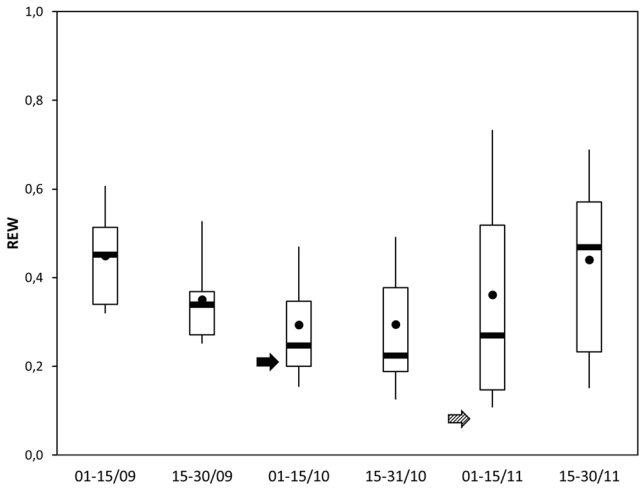

Fig. 4 Box plots showing the bi-monthly variation in relative extractable water (REW) from 2004 to 2018. Boxes show the mean (black dots), median (horizontal bar), 25th and 75th percentiles; error bars show the 10th and 90th percentiles. Mean REW values when measurements of dry season midday leaf water potential were conducted for 2018 (our study; black arrow) and 2008 (Stahl et al. 2010, dashed arrow) are shown

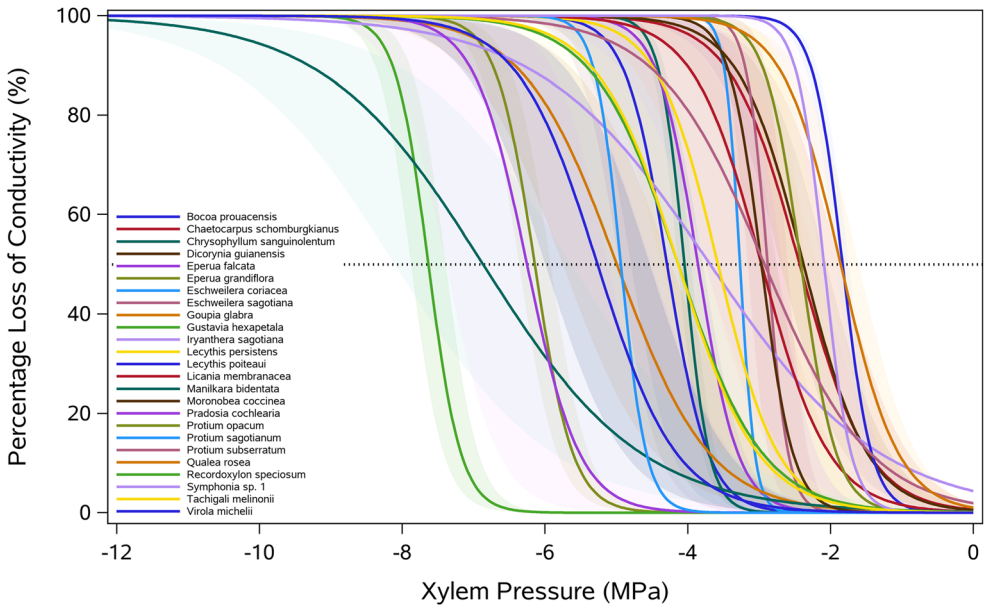

Fig. 5 Mean vulnerability curves for 25 co-occurring species showing the percentage of loss of hydraulic conductivity (%) in the xylem as a function of xylem pressure (Mpa). Shaded bands represent standard errors and 50% loss in conductivity is indicated by a horizontal dotted line

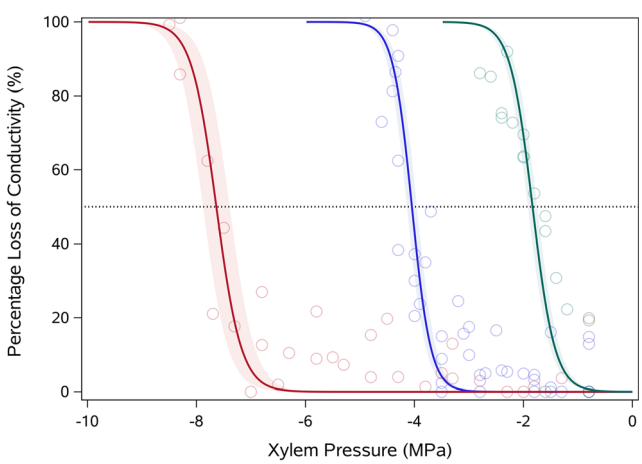

Fig. 6 Mean vulnerability curves for three species showing the percentage of loss of hydraulic conductivity (%) in the xylem as a function of xylem pressure (Mpa). Open circles represent raw data; shaded bands represent standard errors; and a 50% loss in conductivity is indicated by a horizontal dotted line for *Gustavia hexapetala* (red; n = 3), the most resistant species in our dataset, *Chrysophyllum sanguinolentum* (blue; n = 5), an intermediately-resistant species, and *Lecythis poiteaui* (green; n = 4), the least resistant species

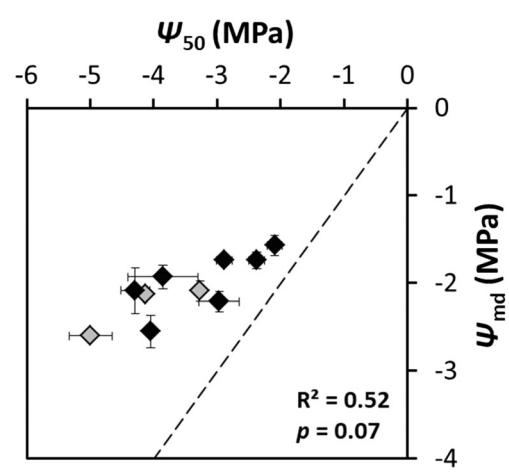

Fig. 7 Relationships between Ψ_{50}, the water potential at 50% loss of branch hydraulic conductivity (Ψ_{50}; MPa), and midday leaf water potential measured during the severe dry season of 2008 (Ψ_{md}; MPa) for 10 canopy-tree species sampled in French Guiana (black $n \geq 3$; gray $n < 3$). All error bars represent standard errors of the mean. The 1:1 line (dashed line) is represented. Coefficients of determination (R^2) and significance levels (p) are shown

References

Adams HD, Zeppel MJB, Anderegg WRL, Hartmann H, Landhäusser SM, Tissue DT, Huxman TE, Hudson PJ, Franz TE, Allen CD, Anderegg LDL, Barron-Gafford GA, Beerling DJ, Breshears DD, Brodribb TJ, Bugmann H, Cobb RC, Collins AD, Dickman LT, Duan H, Ewers BE, Galiano L, Galvez DA, Garcia-Forner N, Gaylord ML, Germino MJ, Gessler A, Hacke UG, Hakamada R, Hector A, Jenkins MW, Kane JM, Kolb TE, Law DJ, Lewis JD, Limousin J-M, Love DM, Macalady AK, Martínez-Vilalta J, Mencuccini M, Mitchell PJ, Muss JD, O'Brien MJ, O'Grady AP, Pangle RE, Pinkard EA, Piper FI, Plaut JA, Pockman WT, Quirk J, Reinhardt K, Ripullone F, Ryan MG, Sala A, Sevanto S, Sperry JS, Vargas R, Vennetier M, Way DA, Xu C, Yepez EA, McDowell NG (2017) A multi-species synthesis of physiological mechanisms in drought-induced tree mortality. Nat Ecol Evol 1:1285–1291. https://doi.org/10.1038/s41559-017-0248-x

Aguilos M, Stahl C, Burban B, Hérault B, Courtois E, Coste S, Wagner F, Ziegler C, Takagi K, Bonal D (2019) Interannual and seasonal variations in ecosystem transpiration and water use efficiency in a tropical rainforest. Forests 10:14. https://doi.org/10.3390/f10010014

Anderegg WRL, Flint A, C-y H, Flint L, Berry JA, Davis FW, Sperry JS, Field CB (2015) Tree mortality predicted from drought-induced vascular damage. Nat Geosci 8:367. https://doi.org/10.1038/ngeo2400

Anderegg WR, Klein T, Bartlett M, Sack L, Pellegrini AF, Choat B, Jansen S (2016) Meta-analysis reveals that hydraulic traits explain cross-species patterns of drought-induced tree mortality across the globe. Proc Natl Acad Sci 113:5024–5029. https://doi.org/10.1073/pnas.1525678113

Bartlett MK, Scoffoni C, Ardy R, Zhang Y, Sun S, Cao K, Sack L (2012a) Rapid determination of comparative drought tolerance traits: using an osmometer to predict turgor loss point. Methods Ecol Evol 3: 880–888. https://doi.org/10.1111/j.2041-210X.2012.00230.x

Bartlett MK, Scoffoni C, Sack L (2012b) The determinants of leaf turgor loss point and prediction of drought tolerance of species and biomes: a global meta-analysis. Ecol Lett 15:393–405. https://doi.org/10.1111/j.1461-0248.2012.01751.x

Bartlett MK, Klein T, Jansen S, Choat B, Sack L (2016) The correlations and sequence of plant stomatal, hydraulic, and wilting responses to drought. Proc Natl Acad Sci 113:13098–13103. https://doi.org/10.1073/pnas.1604088113

Bennett AC, McDowell NG, Allen CD, Anderson-Teixeira KJ (2015) Larger trees suffer most during drought in forests worldwide. Nat Plants 1:15139. https://doi.org/10.1038/nplants.2015.139

Bonal D, Burban B, Stahl C, Wagner F, Herault B (2016) The response of tropical rainforests to drought-lessons from recent research and future prospects. Ann For Sci 73:27–44. https://doi.org/10.1007/s13595-015-0522-5

Brodribb TJ (2017) Progressing from 'functional' to mechanistic traits. The New phytologist 215:9–11. https://doi.org/10.1111/nph.14620

Brodribb TJ, Holbrook NM, Edwards EJ, Gutierrez MV (2003) Relations between stomatal closure, leaf turgor and xylem vulnerability in eight tropical dry forest trees. Plant Cell Environ 26:443–450. https://doi.org/10.1046/j.1365-3040.2003.00975.x

Choat B, Sack L, Holbrook NM (2007) Diversity of hydraulic traits in nine Cordia species growing in tropical forests with contrasting precipitation. The New phytologist 175:686–698. https://doi.org/10.1111/j.1469-8137.2007.02137.x

Choat B, Jansen S, Brodribb TJ, Cochard H, Delzon S, Bhaskar R, Bucci SJ, Feild TS, Gleason SM, Hacke UG, Jacobsen AL, Lens F, Maherali H, Martinez-Vilalta J, Mayr S, Mencuccini M, Mitchell PJ, Nardini A, Pittermann J, Pratt RB, Sperry JS, Westoby M, Wright IJ, Zanne AE (2012) Global convergence in the vulnerability of forests to drought. Nature 491:752–755. https://doi.org/10.1038/nature11688

Choat B, Brodribb TJ, Brodersen CR, Duursma RA, Lopez R, Medlyn BE (2018) Triggers of tree mortality under drought. Nature 558: 531–539. https://doi.org/10.1038/s41586-018-0240-x

Christoffersen BO, Gloor M, Fauset S, Fyllas NM, Galbraith DR, Baker TR, Kruijt B, Rowland L, Fisher RA, Binks OJ, Sevanto S, Xu C, Jansen S, Choat B, Mencuccini M, McDowell NG, Meir P (2016) Linking hydraulic traits to tropical forest function in a size-structured and trait-driven model (TFS v.1-Hydro). Geosci Model Dev 9:4227–4255. https://doi.org/10.5194/gmd-9-4227-2016

Cochard H, Delzon S (2013) Hydraulic failure and repair are not routine in trees. Ann For Sci 70:659–661. https://doi.org/10.1007/s13595-013-0317-5

Cochard H, Badel E, Herbette S, Delzon S, Choat B, Jansen S (2013) Methods for measuring plant vulnerability to cavitation: a critical review. J Exp Bot 64:4779–4791. https://doi.org/10.1093/jxb/ert193

Creek D, Blackman CJ, Brodribb TJ, Choat B, Tissue DT (2018) Coordination between leaf, stem, and root hydraulics and gas exchange in three arid-zone angiosperms during severe drought and recovery. Plant Cell Environ 41:2869–2881. https://doi.org/10.1111/pce.13418

Delzon S (2015) New insight into leaf drought tolerance. Funct Ecol 29: 1247–1249. https://doi.org/10.1111/1365-2435.12500

Delzon S, Cochard H (2014) Recent advances in tree hydraulics highlight the ecological significance of the hydraulic safety margin. The New phytologist 203:355–358. https://doi.org/10.1111/nph.12798

Delzon S, Douthe C, Sala A, Cochard H (2010) Mechanism of water-stress induced cavitation in conifers: bordered pit structure and function support the hypothesis of seal capillary-seeding. Plant Cell Environ 33:2101–2111. https://doi.org/10.1111/j.1365-3040.2010.02208.x

Duffy PB, Brando P, Asner GP, Field CB (2015) Projections of future meteorological drought and wet periods in the Amazon. Proc Natl Acad Sci 112:13172–13177. https://doi.org/10.1073/pnas.1421010112

Duursma RA, Blackman CJ, Lopez R, Martin-StPaul NK, Cochard H, Medlyn BE (2019) On the minimum leaf conductance: its role in models of plant water use, and ecological and environmental controls. The New phytologist 221:693–705. https://doi.org/10.1111/nph.15395

Esquivel-Muelbert A, Dexter KG, Lewis SL, Brienen RJW, Feldpausch TR, Lloyd J, Monteagudo-Mendoza A, Arroyo L, Alvarez-Davila E, Higuchi N, Marimon BS, Marimon-Junior BH, Silveira M, Vilanova E, Gloor E, Malhi Y, Chave J, Barlow J, Bonal D, Davila Cardozo N, Erwin T, Fauset S, Herault B, Laurance S, Poorter L, Qie L, Stahl C, Sullivan MJP, Ter Steege H, Vos VA, Zuidema PA, Almeida E, Almeida de Oliveira E, Andrade A, Vieira SA, Aragao L, Araujo-Murakami A, Arets E, Aymard CG, Baraloto C, Camargo PB, Barroso JG, Bongers F, Boot R, Camargo JL, Castro W, Chama Moscoso V, Comiskey J, Cornejo Valverde F, Lola da Costa AC, Del Aguila Pasquel J, Di Fiore A, Fernanda Duque L, Elias F, Engel J, Flores Llampazo G, Galbraith D, Herrera Fernandez R, Honorio Coronado E, Hubau W, Jimenez-Rojas E, Lima AJN, Umetsu RK, Laurance W, Lopez-Gonzalez G, Lovejoy T, Aurelio Melo Cruz O, Morandi PS, Neill D, Nunez Vargas P, Pallqui Camacho NC, Parada Gutierrez A, Pardo G,

Peacock J, Pena-Claros M, Penuela-Mora MC, Petronelli P, Pickavance GC, Pitman N, Prieto A, Quesada C, Ramirez-Angulo H, Rejou-Mechain M, Restrepo Correa Z, Roopsind A, Rudas A, Salomao R, Silva N, Silva Espejo J, Singh J, Stropp J, Terborgh J, Thomas R, Toledo M, Torres-Lezama A, Valenzuela Gamarra L, van de Meer PJ, van der Heijden G, van der Hout P, Vasquez Martinez R, Vela C, Vieira ICG, Phillips OL (2019) Compositional response of Amazon forests to climate change. Glob Chang Biol 25:39–56. https://doi.org/10.1111/gcb.14413

Ewers FW, Fisher JB (1989) Techniques for measuring vessel lengths and diameters in stems of woody plants. Am J Bot 76:645–656. https://doi.org/10.1002/j.1537-2197.1989.tb11360.x

Fargeon H, Aubry-Kientz M, Brunaux O, Descroix L, Gaspard R, Guitet S, Rossi V, Hérault B (2016) Vulnerability of commercial tree species to water stress in logged forests of the Guiana Shield. Forests 7: 105. https://doi.org/10.3390/f7050105

Fisher RA, Williams M, Do Vale RL, Da Costa AL, Meir P (2006) Evidence from Amazonian forests is consistent with isohydric control of leaf water potential. Plant Cell Environ 29:151–165. https://doi.org/10.1111/j.1365-3040.2005.01407.x

Hochberg U, Rockwell FE, Holbrook NM, Cochard H (2018) Iso/Anisohydry: A Plant-Environment Interaction Rather Than a Simple Hydraulic Trait. Trends Plant Sci 23:112–120. https://doi.org/10.1016/j.tplants.2017.11.002

Jacobsen AL, RB Pratt, MF Tobin, UG Hacke, FW Ewers (2012) A global analysis of xylem vessel length in woody plants. American Journal of Botany 99:1583-1591. https://doi.org/10.3732/ajb.1200140

Jones HG, Sutherland RA (1991) Stomatal control of xylem embolism. Plant Cell Environ 14:607–612. https://doi.org/10.1111/j.1365-3040.1991.tb01532.x

Lobo A, Torres-Ruiz JM, Burlett R, Lemaire C, Parise C, Francioni C, Truffaut L, Tomaskova I, Hansen JK, Kjaer ED, Kremer A, Delzon S (2018) Assessing inter- and intraspecific variability of xylem vulnerability to embolism in oaks. For Ecol Manag 424:53–61. https://doi.org/10.1016/j.foreco.2018.04.031

Machado J-L, Tyree MT (1994) Patterns of hydraulic architecture and water relations of two tropical canopy trees with contrasting leaf phenologies: Ochroma pyramidale and Pseudobombax septenatum. Tree Physiol 14:219–240. https://doi.org/10.1093/treephys/14.3.219

Maherali H, Pockman WT, Jackson RB (2004) Adaptive variation in the vulnerability of woody plants to xylem cavitation. Ecology 85: 2184–2199. https://doi.org/10.1890/02-0538

Marechaux I, Bartlett MK, Sack L, Baraloto C, Engel J, Joetzjer E, Chave J (2015) Drought tolerance as predicted by leaf water potential at turgor loss point varies strongly across species within an Amazonian forest. Funct Ecol 29:1268–1277. https://doi.org/10.1111/1365-2435.12452

Maréchaux I, Bartlett MK, Gaucher P, Sack L, Chave J (2016) Causes of variation in leaf-level drought tolerance within an Amazonian forest. J Plant Hydraul 3:e004. https://doi.org/10.20870/jph.2016.e004

Martin-StPaul N, Delzon S, Cochard H (2017) Plant resistance to drought depends on timely stomatal closure. Ecol Lett 20:1437–1447. https://doi.org/10.1111/ele.12851

Mayle FE, Power MJ (2008) Impact of a drier Early-Mid-Holocene climate upon Amazonian forests. Philos Trans R Soc Lond Ser B Biol Sci 363:1829–1838. https://doi.org/10.1098/rstb.2007.0019

Meinzer FC, Woodruff DR, Domec JC, Goldstein G, Campanello PI, Gatti MG, Villalobos-Vega R (2008) Coordination of leaf and stem water transport properties in tropical forest trees. Oecologia 156:31–41. https://doi.org/10.1007/s00442-008-0974-5

Meinzer FC, Johnson DM, Lachenbruch B, McCulloh KA, Woodruff DR (2009) Xylem hydraulic safety margins in woody plants: coordination of stomatal control of xylem tension with hydraulic capacitance. Funct Ecol 23:922–930. https://doi.org/10.1111/j.1365-2435.2009.01577.x

Mencuccini M, Minunno F, Salmon Y, Martinez-Vilalta J, Holtta T (2015) Coordination of physiological traits involved in drought-induced mortality of woody plants. The New phytologist 208:396–409. https://doi.org/10.1111/nph.13461

Nolf M, Creek D, Duursma R, Holtum J, Mayr S, Choat B (2015) Stem and leaf hydraulic properties are finely coordinated in three tropical rain forest tree species. Plant Cell Environ 38:2652–2661. https://doi.org/10.1111/pce.12581

Oliveira RS, Costa FRC, van Baalen E, de Jonge A, Bittencourt PR, Almanza Y, Barros FV, Cordoba EC, Fagundes MV, Garcia S, Guimaraes ZTM, Hertel M, Schietti J, Rodrigues-Souza J, Poorter L (2019) Embolism resistance drives the distribution of Amazonian rainforest tree species along hydro-topographic gradients. The New phytologist 221:1457–1465. https://doi.org/10.1111/nph.15463

Pammenter NW, Vander Willigen C (1998) A mathematical and statistical analysis of the curves illustrating vulnerability of xylem to cavitation. Tree Physiol 18:589–593. https://doi.org/10.1093/treephys/18.8-9.589

Phillips OL, van der Heijden G, Lewis SL, Lopez-Gonzalez G, Aragao L, Lloyd J, Malhi Y, Monteagudo A, Almeida S, Davila EA, Amaral I, Andelman S, Andrade A, Arroyo L, Aymard G, Baker TR, Blanc L, Bonal D, de Oliveira ACA, Chao KJ, Cardozo ND, da Costa L, Feldpausch TR, Fisher JB, Fyllas NM, Freitas MA, Galbraith D, Gloor E, Higuchi N, Honorio E, Jimenez E, Keeling H, Killeen TJ, Lovett JC, Meir P, Mendoza C, Morel A, Vargas PN, Patino S, Peh KSH, Cruz AP, Prieto A, Quesada CA, Ramirez F, Ramirez H, Rudas A, Salamao R, Schwarz M, Silva J, Silveira M, Slik JWF, Sonke B, Thomas AS, Stropp J, Taplin JRD, Vasquez R, Vilanova E (2010) Drought-mortality relationships for tropical forests. New Phytol 187:631–646. https://doi.org/10.1111/j.1469-8137.2010.03359.x

Pivovaroff AL, Sack L, Santiago LS (2014) Coordination of stem and leaf hydraulic conductance in southern California shrubs: a test of the hydraulic segmentation hypothesis. The New phytologist 203:842–850. https://doi.org/10.1111/nph.12850

Pivovaroff AL, Pasquini SC, De Guzman ME, Alstad KP, Stemke JS, Santiago LS, Field K (2016) Multiple strategies for drought survival among woody plant species. Funct Ecol 30:517–526. https://doi.org/10.1111/1365-2435.12518

Powell TL, Wheeler JK, de Oliveira AAR, da Costa ACL, Saleska SR, Meir P, Moorcroft PR (2017) Differences in xylem and leaf hydraulic traits explain differences in drought tolerance among mature Amazon rainforest trees. Glob Chang Biol 23:4280–4293. https://doi.org/10.1111/gcb.13731

Rowland L, da Costa AC, Galbraith DR, Oliveira RS, Binks OJ, Oliveira AA, Pullen AM, Doughty CE, Metcalfe DB, Vasconcelos SS, Ferreira LV, Malhi Y, Grace J, Mencuccini M, Meir P (2015) Death from drought in tropical forests is triggered by hydraulics not carbon starvation. Nature 528:119–122. https://doi.org/10.1038/nature15539

Santiago LS, Bonal D, De Guzman ME, Avila-Lovera E (2016) Drought Survival Strategies of Tropical Trees. In: Goldstein G, Santiago LS (eds) Tropical Tree Physiology: Adaptations and Responses in a Changing Environment, pp 243–258

Santiago LS, De Guzman ME, Baraloto C, Vogenberg JE, Brodie M, Herault B, Fortunel C, Bonal D (2018) Coordination and trade-offs among hydraulic safety, efficiency and drought avoidance traits in Amazonian rainforest canopy tree species. New Phytol 218: 1015–1024. https://doi.org/10.1111/nph.15058

Scoffoni C, Albuquerque C, Brodersen CR, Townes SV, John GP, Bartlett MK, Buckley TN, McElrone AJ, Sack L (2017) Outside-Xylem Vulnerability, Not Xylem Embolism, Controls Leaf Hydraulic Decline during Dehydration. Plant Physiol 173:1197–1210. https://doi.org/10.1104/pp.16.01643

Sperry JS, Tyree MT, Donnelly JR (1988) Vulnerability of xylem to embolism in a mangrove vs an inland species of Rhizophoraceae.

Physiol Plant 74:276–283. https://doi.org/10.1111/j.1399-3054.1988.tb00632.x

Sperry JS, Hacke UG, Feild TS, Sano Y, Sikkema EH (2007) Hydraulic consequences of vessel evolution in angiosperms. Int J Plant Sci 168:1127–1139. https://doi.org/10.1086/520726

Stahl C, Burban B, Bompy F, Jolin ZB, Sermage J, Bonal D (2010) Seasonal variation in atmospheric relative humidity contributes to explaining seasonal variation in trunk circumference of tropical rainforest trees in French Guiana. J Trop Ecol 26:393–405. https://doi.org/10.1017/s0266467410000155

Stahl C, Burban B, Wagner F, Goret J-Y, Bompy F, Bonal D (2013) Influence of seasonal variations in soil water availability on gas exchange of tropical canopy trees. Biotropica 45:155–164. https://doi.org/10.1111/j.1744-7429.2012.00902.x

Torres-Ruiz JM, Cochard H, Delzon S (2016) Why do trees take more risks in the Amazon? Journal of Plant Hydraulics 3:e005. https://doi.org/10.20870/jph.2016.e005

Tyree MT, Patiño S, Becker P (1998) Vulnerability to drought-induced embolism of Bornean heath and dipterocarp forest trees. Tree Physiol 18:583–588. https://doi.org/10.1093/treephys/18.8-9.583

Urli M, Porte AJ, Cochard H, Guengant Y, Burlett R, Delzon S (2013) Xylem embolism threshold for catastrophic hydraulic failure in angiosperm trees. Tree Physiol 33:672–683. https://doi.org/10.1093/treephys/tpt030

Wagner F, Rossi V, Stahl C, Bonal D, Hérault B (2012) Water availability is the main climate driver of neotropical tree growth. PLoS One 7: e34074. https://doi.org/10.1371/journal.pone.0034074

Wagner F, Rossi V, Stahl C, Bonal D, Hérault B (2013) Asynchronism in leaf and wood production in tropical forests: a study combining satellite and ground-based measurements. Biogeosciences 10: 7307–7321. https://doi.org/10.5194/bg-10-7307-2013

Zhu S-D, Liu H, Xu Q-Y, Cao K-F, Ye Q, Poorter L (2016) Are leaves more vulnerable to cavitation than branches? Funct Ecol 30:1740–1744. https://doi.org/10.1111/1365-2435.12656

Zhu SD, Chen YJ, Ye Q, He PC, Liu H, Li RH, Fu PL, Jiang GF, Cao KF (2018) Leaf turgor loss point is correlated with drought tolerance and leaf carbon economics traits. Tree Physiol 38:658–663. https://doi.org/10.1093/treephys/tpy013

Affiliations

Camille Ziegler[1,2] · Sabrina Coste[3] · Clément Stahl[2] · Sylvain Delzon[4] · Sébastien Levionnois[5] · Jocelyn Cazal[2] · Hervé Cochard[6] · Adriane Esquivel-Muelbert[7,8] · Jean-Yves Goret[2] · Patrick Heuret[9] · Gaëlle Jaouen[10] · Louis S. Santiago[11,12] · Damien Bonal[1]

1 Université de Lorraine, AgroParisTech, INRAE, UMR Silva, 54000 Nancy, France

2 INRAE, UMR EcoFoG, AgroParisTech, Cirad, CNRS, Université des Antilles, Université de Guyane, 97310 Kourou, France

3 Université de Guyane, UMR EcoFoG, AgroParisTech, Cirad, CNRS, INRAE, Université des Antilles, 97310 Kourou, France

4 INRA, University of Bordeaux, UMR BIOGECO, 33615 Pessac, France

5 CNRS, UMR EcoFoG, AgroParisTech, Cirad, CNRS, INRAE, Université des Antilles, Université de Guyane, 97310 Kourou, France

6 Université Clermont-Auvergne, INRAE, PIAF, 63000 Clermont-Ferrand, France

7 School of Geography, University of Leeds, Leeds, UK

8 School of Geography, Environment and Earth Sciences, University of Birmingham, Birmingham, UK

9 AMAP, Univ Montpellier, CIRAD, CNRS, INRAE, IRD, Montpellier, France

10 AgroParisTech, UMR EcoFoG, Cirad, CNRS, INRAE, Université des Antilles, Université de Guyane, 97310 Kourou, France

11 Department of Botany & Plant Sciences, University of California, Riverside, CA 92521, USA

12 Smithsonian Tropical Research Institute, Balboa, Ancon, Republic of Panama